Local Mean Decomposition, using an Empirical Optimal Envelope and a Log-Envelope, for Bearing Fault Detection

Bouaouiche Karim, Menasria Yamina, Khalfa Dalila

Electromechanical Engineering Laboratory, Badji Mokhtar University-Annaba B.P.12, 23000 Annaba, Algeria, e-mail: karim.bouaouiche@univ-annaba.dz, yamina.menasria@univ-annaba.dz, dalila.khalfa@univ-annaba.dz

Abstract: The analysis of bearing vibration signals is presented in this study, using a proposed approach that combines several signal processing tools. Starting with the local mean decomposition using an empirical optimal envelope algorithm to decompose the signal into several components. We then select the relevant components related to defects, which include high energy pulses, using a new indicator called defect symptom. Then, a new signal is reconstructed by adding the previously selected effective components. Peaks can be observed at the fault frequency of component in the log-envelope autocorrelation spectrum of the new signal. After applying the approach to the signals available in the Case Western Reserve University and Paderborn University databases, peaks were observed at the respective inner and outer race fault frequencies.

Keywords: bearing; vibration signal; fault frequency; energy; pulses

1 Introduction

In all rotating machinery, the bearing has an essential function of supporting loads and facilitating movement between shafts. Hence, inadequate installation or overloading may cause malfunctions in bearing components, such as the inner or outer ring, cage, and balls. The bearing is situated inside the machine and if it fails, the machine performance is reduced, necessitating the monitoring of the bearing condition. The techniques used to detect faults can be classified into two categories: the first relies on signal analysis, while the second is based on evaluating the behavior of a detailed model of the machine operating system [1].

Vibration signal analysis is a highly effective approach to machinery monitoring, which entails measuring and interpreting vibrations using sensors and analyzers [2]. Vibrations are collected either periodically or continuously, and the condition is monitored by comparing the results with reference data from a bearing or

machine in a healthy state [2]. Signal processing methods are essential for fault detection [2]. Such as envelope analysis is the most popular method for obtaining valuable information about bearings from vibration signals [3]. To detect faults in bearings, various techniques are employed, including de-convolution, decomposition, and stationary cycle analysis [4]. The presence of pulses in the vibration signal serves as symptoms of these defects [4]. Signal impulses, such as those found in a failed bearing, are often identified using kurtosis values greater than three [5]. An essential step in identifying the impulse section of a signal is to decompose the signal and add up the modes that have kurtosis values exceeding three [5].

To diagnose rotating machinery, the vibration signal is often examined because of a complex process between the impulse component, which is linked to the fault, and the transfer function of the path between the fault source and the sensor [6]. Deconvolution is an inverse operation of convolution used to eliminate noise and extract the impulse part of the signal [7]. This technique is widely applied in this field [7].

We present in our paper an approach that utilizes various signal processing algorithms to analyze the vibration signals of the bearing. The identification and localization of the faulty components are achieved through the reconstruction of a new signal from the original signal. The remainder of the article is organized as follows: section (2) presents the proposed approach to bearing defect detection, as well as the different signal processing methods incorporated in this approach, which are presented in the subsections. Section (3) comprises the experimental study consisting of the analysis of vibration signals available in two different databases, in order to evaluate the effectiveness of the proposed approach from the results obtained. Finally, we present our conclusions.

2 Methods

In this section, we propose an approach based on signal processing methods, demonstrated in the subsections below. Figure (1) shows the flowchart of the approach.

The steps of the proposed approach are illustrated as follows:

- The local mean decomposition using an empirical optimal envelope (EOE-LMD) algorithm is used to decompose the signal into several components (PF).
- The indicator symptom of defect (SD) is calculated for each component.
- If SD is greater than 40.62, the component (PF) is selected, otherwise, it is eliminated.

- Reconstruction of new signal:

$$nx(t) = \sum PF(t) \quad With \quad SD \geq 40.62 \tag{1}$$

- Log-envelope spectrum of autocorrelation of the new signal.

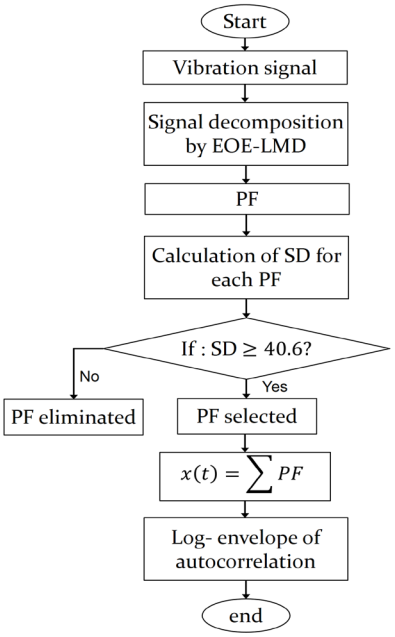

Figure 1
Flowchart of the approach

2.1 Local Mean Decomposition using an Empirical Optimal Envelope

The empirical optimal envelope (EOE) method is integrated into the local mean decomposition (LMD) algorithm to decompose a signal into multiple components (PF) [8]. Additionally, two interpolation functions cubic spline (CS) and piecewise cubic Hermite interpolating polynomial (PCHIP) are included to improve signal decomposition convergence [8].

The EOE method optimizes the envelope distance to approximate the ideal envelope, and reference [8] provides information on the various steps of the EOE algorithm.

The EOE-LMD algorithm is comprised of the following steps [8]:

1) Take the signal $x(t)$ as input and initialize a counting variable C=1.

2) The interpolation function chosen depends on the value of C. If C=1, cubic spline (CS) is used, while for C>1, the piecewise cubic Hermite interpolating polynomial (PCHIP) is adopted.

The EOE algorithm is used to calculate the lower $e_l(t)$ and upper, $e_u(t)$ envelopes, the local average $m_{11}(t)$ and local envelope $a_{11}(t)$ functions can be obtained using the following equations:

$$m_{11}(t) = \frac{e_l(t) + e_u(t)}{2} \tag{2}$$

$$a_{11}(t) = \frac{e_u(t) - e_l(t)}{2} \tag{3}$$

3) The following formula is used to calculate the modulated signal:

$$s_{11}(t) = \frac{x(t) - m_{11}(t)}{a_{11}(t)} \tag{4}$$

Let C=C+1, the signal $s_{11}(t)$ can be regarded as a new signal. If $a_{12}(t) = 1$, $s_{11}(t)$ therefore is a purely normalized modulated signal and the first component PF1 is obtained. If $a_{12}(t) \neq 1$, steps 2 and 3 are repeated until the envelope function $a_{1(n+1)}(t)$ of $s_{1n}(t)$ equal 1.

4) The envelope signal is obtained by multiplying all envelope functions:

$$a_1(t) = a_{11}(t)a_{12}(t).....a_{1n}(t) \tag{5}$$

The first component PF1 is obtained by multiplying the envelope signals $a_1(t)$ and $s_{1n}(t)$.

$$PF1(t) = a_1(t) \times s_{1n}(t) \tag{6}$$

5) The first residual $u_1(t)$ is obtained by subtracting PF1 from the original signal $x(t)$ and considering it as a new signal.

$$u_1(t) = x(t) - PF1(t) \tag{7}$$

Steps 1, 2, 3, and 4 are repeated until the k[th] residual becomes constant.

Finally, the original signal is decomposed into several components (PF) and the residual:

$$x(t) = u_k + \sum_{i=1}^{k} PF_i(t) \tag{8}$$

2.2 Symptoms of Defects

Pulses in the signals and the increase of energy at a certain frequency are two symptoms indicating the presence of defects in the bearings [9]. Therefore, we suggest an indicator called defect symptom (SD) to assess the pulses and high energy. SD is computed as the product of the Gini index (GI) and the signal energy (E), as shown in the equation:

$$SD = GI \times E \tag{9}$$

The Gini index (GI) is a statistical parameter used to evaluate the impulsiveness of signals created by defects [10]. The values of GI range between 0 and 1, and it is defined by the following formula [11]:

$$GI(x) = 1 - 2\sum \frac{|x_k|}{x_1} \times \left(\frac{N - k + 0.5}{N} \right) \tag{10}$$

The elements of the signal are denoted by (x_k) and reorganized as follows [11]:

$$|x_1| \le |x_2| \le,....,\le |x_N| \tag{11}$$

The Gini index is more effective than kurtosis in detecting repetitive pulses [12]. When the signal contains a pulse train, the Gini index attains their maximum value, while in the opposite scenario, it takes on a minimum value [12].

The energy of the vibration signal is defined by equation (12) as follows [13]:

$$E = \int_{-\infty}^{+\infty} |x(t)|^2 dt \tag{12}$$

The vibration signals of a bearing will be analyzed during a test, both in a healthy state and a failed state with inner ring and ball damage and a defect size of 0.3556 mm. The signals being used are from the Case Western Reserve University database and were collected at a sampling frequency of 12 kHz. The goal of the test is to define the threshold of SD danger. As a result, the figure (2) shows the variation of SD as a function of speed and load.

From the values of SD, it can be observed that the signals of the healthy state have values lower than 32.5, while the signals of the faulty state exhibit very high values. Based on this test, a threshold for SD can be defined as follows:

$$SD_{Threshold} = 1.25 \times 32.5 \Leftrightarrow SD_{Threshold} = 40.62 \tag{13}$$

If: $SD \ge 40.62$ bearing failure

Else: a healthy bearing

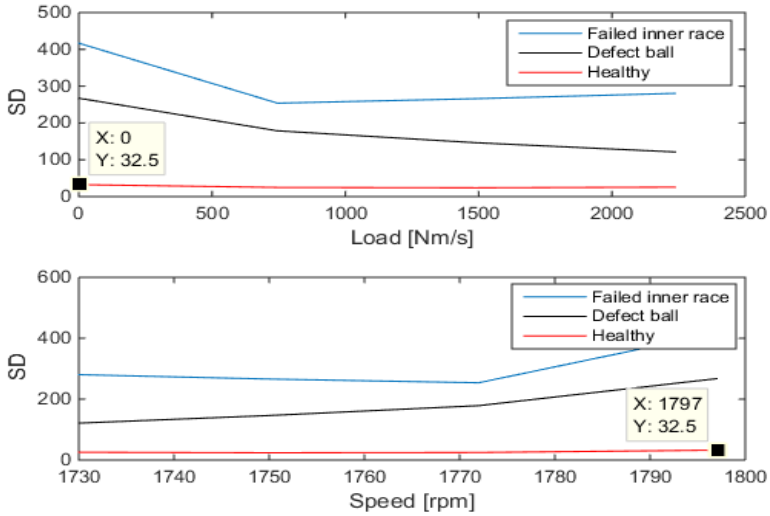

Figure 2
Variation of SD

2.3 Log-Envelope Spectrum of Autocorrelation

The envelope spectrum of a signal can be calculated using the Fourier and Hilbert transform, which is commonly used for detecting mechanical defects [14]. This method facilitates the extraction of the faulty component frequency [14].

An effective method in processing vibration signals is the autocorrelation function, which reduces noise and enhances the impulsive periodic part of the signal [15]. Autocorrelation, on the other hand, measures the similarity between a signal and its time-shifted variant [16]. The vibration signal can be represented as a combination of impulsive periodic (p) and noise components (n) [16]:

$$x(t) = p(t) + n(t) \tag{14}$$

The autocorrelation calculation of the signal is expressed as follows [16]:

$$R_{xx}(\tau) = \int_{-\infty}^{+\infty} x(t+\tau)x(t)dt \tag{15}$$

$$R_{xx}(\tau) = R_{pp}(\tau) + R_{pn}(\tau) + R_{np}(\tau) + R_{nn}(\tau) \tag{16}$$

$R_{pp}(\tau)$ $R_{nn}(\tau)$
$R_{np}(\tau)$ and $R_{pn}(\tau)$ represent the cross-correlation between (n) and (p).

The components (p) and (n) are independent, therefore $R_{np}(\tau)=0$ and $R_{pn}(\tau)=0$. The autocorrelation of white noise is theoretically zero $R_{nn}(\tau)=0$, so it can be concluded that:

$$R_{xx}(\tau)\cong R_{pp}(\tau) \tag{17}$$

The equations presented above express the process of applying the log envelope on the autocorrelation of the vibration signal [17]:

$$H[R(t)]=R(t)*\frac{1}{\pi t} \tag{18}$$

$$An(t)=R(t)+jH[R(t)] \tag{19}$$

$$Le(t)=Ln(\left|An(t)\right|^2)\Leftrightarrow Le=Ln(x(t)^2+H[x(t)]^2) \tag{20}$$

$$Le(f)=\int_{-\infty}^{+\infty}Le(t)e^{-j2\pi ft}dt \tag{21}$$

The log-envelope spectrum of autocorrelation can be used to establish a correlation between the frequency of high amplitude peaks and the frequencies of defects in the bearing components. The defect frequencies are defined by the following formulas [18]:

- Inner race:

$$F_{ir}=\frac{z\times Fr}{2}(1+\frac{d}{Dm}\cos(a)) \tag{22}$$

- Outer race:

$$F_{or}=\frac{z\times Fr}{2}(1-\frac{d}{Dm}\cos(a)) \tag{23}$$

- Cage:

$$F_{c}=\frac{Fr}{2}(1-\frac{d}{Dm}\cos(a)) \tag{24}$$

- Rolling element:

$$F_{re}=\frac{Dm\times Fr}{2d}(1-\frac{d^2}{Dm^2}\cos^2(a)) \tag{25}$$

3 Experimental Study

The effectiveness of the proposed approach was evaluated by analyzing vibration signals from the databases of Case Western Reserve University (CWRU) and Paderborn University.

3.1 Case Western Reserve University Database

MATLAB files containing vibration signals can be obtained from CWRU, which correspond to a motor with two bearings. The first bearing is positioned at the drive end, and the second one is at the fan end, as indicated in the test strip presented in reference [19].

If you are conducting a study and wish to analyze signals from a 6205-2 RS JEM SKF bearing located at the drive end, you can apply the proposed method to two signals that exhibit inner ring defects while the bearing is operating under various conditions, as outlined in the table 2 [19].

The fault frequencies of the rolling elements are obtained by multiplying the operating speed in Hz with the coefficients, which are presented in Table 1 [19].

Table 1
Fault frequencies

Components	**Coefficients**	**Fault frequencies**
Inner race	5.4152	$F_{ir} = 5.4152 \times Fr$
Outer race	3.5848	$F_{or} = 3.5848 \times Fr$
Cage	0.39828	$F_{c} = 0.39828 \times Fr$
Ball	4.7135	$F_{b} = 4.7135 \times Fr$

Table 2
Vibration signals

Operating speed	**Sampling frequency**	**Defect diameter**	**Load**	**Defect frequency**
1772 rpm	12 kHz	0.3556 mm	745.7 Nm/s	159.92 Hz
1730 rpm	12 kHz	0.3556 mm	2237.1 Nm/s	156.13 Hz

3.1.1 Results and Discussions

Case 1: The inner ring fault signal is analyzed while the bearing is rotating at 1730 rpm and under a load 2237.1 Nm/s

- As figure (3) demonstrates, the vibration signal has a complex spectrum, making it challenging to detect defects. The value of SD=280.44, which is significantly higher than the threshold of 40.62, confirms the existence of a defect.
- The figure (4) displays three PF components generated by the EOE-LMD algorithm.
- The values of SD for each component (PF) are shown in table (3), and equation (26) represents the new signal.

$$nx(t) = PF1(t) \tag{26}$$

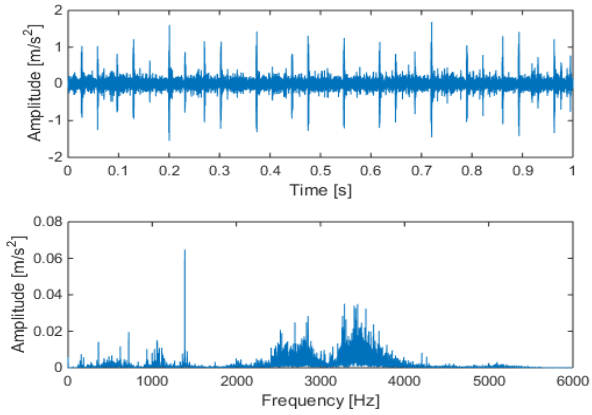

Figure 3
Time and frequency domains of the signal

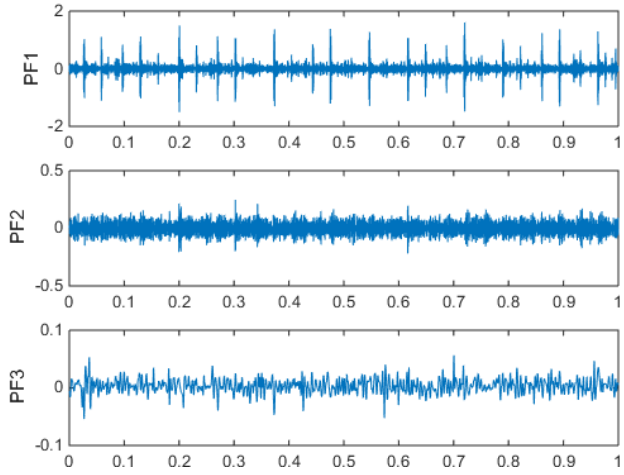

Figure 4
Components (PF)

Table 3
Values of SD

Components	**PF1**	**PF2**	**PF3**
SD	258.4589	15.0068	1.0555

- As shown in figure (5), the autocorrelation log-envelope spectrum of the new signal shows a high amplitude peak at the inner ring fault frequency 156 Hz.

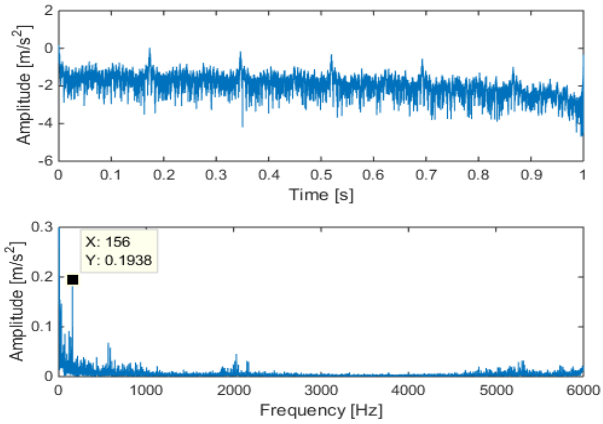

Figure 5
Log-envelope spectrum of autocorrelation

Case 2: By analyzing the fault signal of the inner ring when the bearing rotates at 1772 rpm and under a load of 745.7 Nm/s

- The spectrum of the vibration signal is depicted in figure (6), and it has a value of SD= 253.8264.

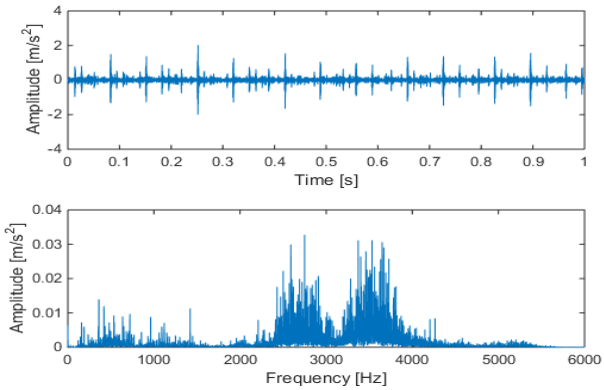

Figure 6
Spectrum of vibration signal

- The EOE-LMD algorithm decomposes the signal into three components. Table (4) shows that the first component has the highest SD value and therefore represents the new signal.

Table 4
Values of SD for each component

Components	**PF1**	**PF2**	**PF3**
SD	245.9514	6.5890	1.0822

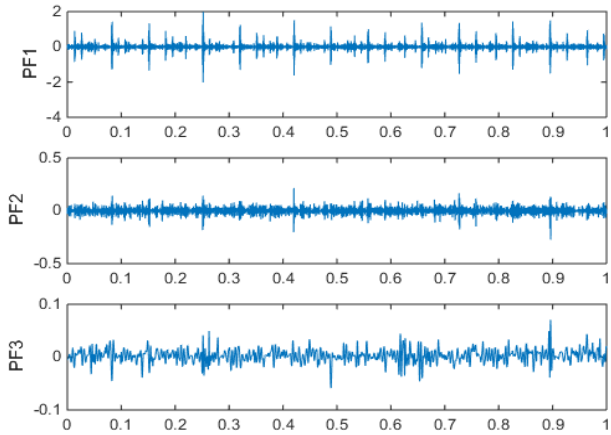

Figure 7
Components (PF) obtained after decomposition

- In the log-envelope autocorrelation spectrum, a prominent peak is detected in the inner ring fault frequency (159.7 Hz), as shown in figure (8).

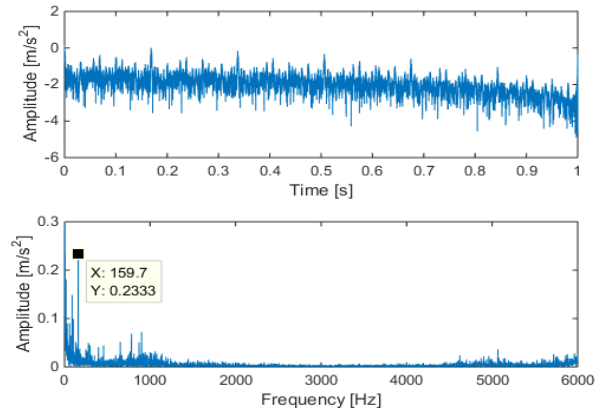

Figure 8
Log-envelope spectrum

3.2 Paderborn University Database

The database contains vibration signals of FAG-6203 ball bearings, and their geometrical parameters are presented in Table (5) [20].

Table 5
Parameters related to geometry

Parameter	**Value**
Diameter of inner race	24 mm
Diameter of outer race	33.1 mm
Pitch diameter	28.55 mm
Ball diameter	6.75 mm
Angle of contact	0°
Number of balls	8

A piezoelectric accelerometer placed on the bearing is used to measure vibration signals, which are then recorded as MATLAB files at a sampling frequency of 64 kHz.

A single vibration signal of outer ring fault is analyzed by the proposed approach. By utilizing the parameters listed in table (5) and applying formula (23), while taking into consideration the operating condition, the fault frequency value is determined.

Table 6
The vibration signal that requires analysis

Operating condition	**Component**	**Fault frequency**
900 rpm/ 1000 N	Outer race	45.81 Hz

3.2.1 Results

- Figure (9) depicts the vibration signal spectrum. SD=2141.2.

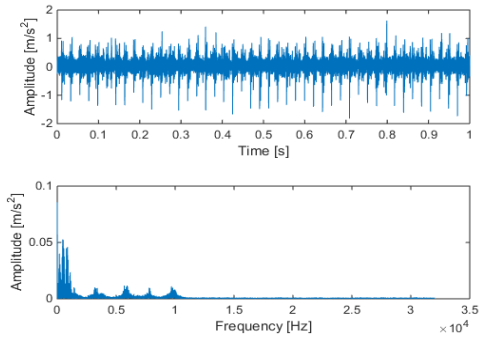

Figure 9
Vibration signal spectrum

- By decomposing the signal, 11 components (PF) were derived, and their corresponding SD values were recorded in the table (7). The equation (27) presents the expression of the new signal.

$$nx(t) = PF_{10}(t) + PF_{11}(t) + \sum_{i=1}^{5} PF_i(t) \tag{27}$$

Table 7
SD values for each PF

PF1	PF2	PF3	PF4	PF5	PF6	PF7	PF8	PF9	PF10	PF11
604.5	275	636.1	407	112.2	36.8	37.5	28.3	21.9	50.4	42.6

- A significant peak corresponding to the fault frequency of the outer ring (45.9 Hz) is present in the autocorrelation log envelope spectrum (Figure 10).

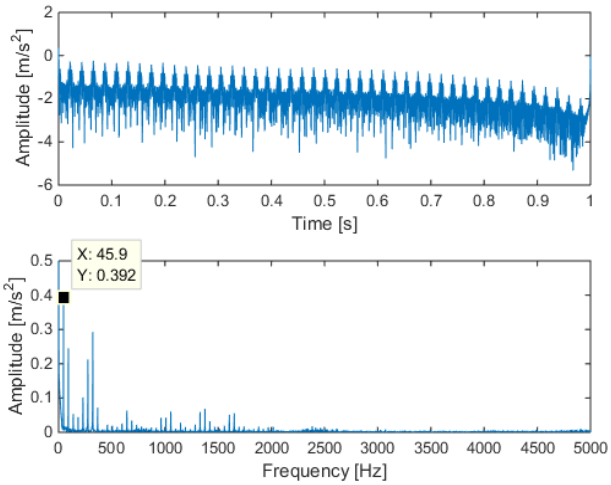

Figure 10
Log-envelope spectrum of autocorrelation of the vibration signal

Conclusions

The proposed approach was applied to vibration signals, available in two different databases, resulting in a good diagnostic outcome. Based on the steps involved in the approach, it can be concluded that:

- The initial vibration signal spectrum is intricate and challenging to interpret, due to the presence of multiple peaks at various frequencies.
- Decomposing a signal is a crucial step in separating useful data. The newly proposed SD indicator has shown greater efficiency in identifying the effective mode composed of high-energy pulses.

- The high amplitude peaks in the spectrum of the log-envelope autocorrelation, allow for the identification of the faulty component based on its frequency.

In addition, the association between signal energy and Gini index is used to evaluate the pulses, thus creating an indicator that enables effective selection of fault symptoms, which are generally present in the form of high-energy pulses.

Thus, on the basis of the peaks of high-energy pulses in the autocorrelation log-envelope spectrum, the fault can be detected by comparing the theoretical fault frequency values with the peak frequency.

References

[1] Zarei, Jafar, Mohammad Amin Tajeddini, and Hamid Reza Karimi. "Vibration analysis for bearing fault detection and classification using an intelligent filter." Mechatronics 24.2 (2014): 151-157

[2] Orhan, Sadettin, Nizami Aktürk, and Veli Celik. "Vibration monitoring for defect diagnosis of rolling element bearings as a predictive maintenance tool: Comprehensive case studies." Ndt & E International 39.4 (2006): 293-298

[3] Moshrefzadeh, Ali, Alessandro Fasana, and Jérôme Antoni. "The spectral amplitude modulation: A nonlinear filtering process for diagnosis of rolling element bearings." Mechanical Systems and Signal Processing 132 (2019): 253-276

[4] Cheng, Yao, Zhiwei Wang, and Weihua Zhang. "Combined Square Envelope Spectrum by Integrating Multiband Bearing Fault Information." IEEE Sensors Journal (2022)

[5] Bouaouiche, Karim, Yamina Menasria, and Dalila Khalfa. "Diagnosis of rotating machine defects by vibration analysis." Acta IMEKO 12.1 (2023): 1-6

[6] Miao, Yonghao, et al. "A review on the application of blind deconvolution in machinery fault diagnosis." Mechanical Systems and Signal Processing 163 (2022): 108202

[7] Buzzoni, Marco, Jérôme Antoni, and Gianluca d'Elia. "Blind deconvolution based on cyclostationarity maximization and its application to fault identification." Journal of Sound and Vibration 432 (2018): 569-601

[8] Jia, Linshan, et al. "The empirical optimal envelope and its application to local mean decomposition." Digital Signal Processing 87 (2019): 166-177

[9] Nishat Toma, Rafia, and Jong-Myon Kim. "Bearing fault classification of induction motors using discrete wavelet transform and ensemble machine learning algorithms." Applied Sciences 10.15 (2020): 5251

[10] Miao, Yonghao, et al. "Practical framework of Gini index in the application of machinery fault feature extraction." Mechanical Systems and Signal Processing 165 (2022): 108333

[11] Nassef, M. G. A., Taha M. Hussein, and Ossama Mokhiamar. "An adaptive variational mode decomposition based on sailfish optimization algorithm and Gini index for fault identification in rolling bearings." Measurement 173 (2021): 108514

[12] Albezzawy, Muhammad N., Mohamed G. Nassef, and Nader Sawalhi. "Rolling element bearing fault identification using a novel three-step adaptive and automated filtration scheme based on Gini index." ISA transactions 101 (2020): 453-460

[13] Colmenero, Alberto Nacer, et al. "Optimization of friction stir spot welding process parameters for Al-Cu dissimilar joints using the energy of the vibration signals." The International Journal of Advanced Manufacturing Technology 100 (2019): 2795-2802

[14] ZHANG, Jian-wen, et al. "A fault diagnosis approach for broken rotor bars based on EMD and envelope analysis." Journal of China University of Mining and Technology 17.2 (2007): 205-209

[15] Xu, Yuandong, et al. "Autocorrelated Envelopes for early fault detection of rolling bearings." Mechanical Systems and Signal Processing 146 (2021): 106990

[16] Pang, Bin, Guiji Tang, and Tian Tian. "Rolling bearing fault diagnosis based on SVDP-based kurtogram and Iterative autocorrelation of Teager energy operator." IEEE access 7 (2019): 77222-77237

[17] Chen, Bingyan, et al. "Product envelope spectrum optimization-gram: An enhanced envelope analysis for rolling bearing fault diagnosis." Mechanical Systems and Signal Processing 193 (2023): 110270

[18] Bouaouiche, Karim, Yamima Menasria, and Dalila Khalifa. "Detection of defects in a bearing by analysis of vibration signals." Diagnostyka 24 (2023)

[19] Case Western Reserve University (CWRU) bearing database. Website: https://engineering.case.edu/bearingdatacenter

[20] Paderborn University bearing database. Website: http://mb.uni-paderborn.de/kat/datacenter

Nomenclature

$An(t)$ – Analytic signal

$a_{11}(t)$ – Local envelope

a – Angle of contact (°)

CWRU – Case Western Reserve University

CS – Interpolation function cubic spline

Dm – Pitch diameter [mm]

d – diameter of the rolling element [mm]

E – Energy

$e_l(t)$ – Lower envelope

$e_u(t)$ – Upper envelope

EOE-LMD– Local mean decomposition using an empirical optimal envelope

F_{ir} – Inner race fault frequency [Hz]

F_c – Cage fault frequency [Hz]

F_{or} – Outer race fault frequency [Hz]

F_{re} – Fault frequency of rolling element [Hz]

Fr – Operating speed [Hz]

FAG – Fischer's automatic steel ball factory

GI – Gini index

H – Hilbert transform

Le – Log-envelope

$Le(f)$ - Log-envelope spectrum

$m_{11}(t)$ – Local average

n – Noise components

$nx(t)$ – New signal

PF – Product function

PCHIP – Piecewise cubic Hermite interpolating polynomial

p – Impulsive periodic

R – Autocorrelation

SD – Symptom of defect

SKF – Swedish ball bearing factory

$s_{11}(t)$ – Modulated signal

u_k – Residual

$x(t)$ – Vibration signal

z – Number of rolling elements